Nanoscale

Accepted Manuscript

This article can be cited before page numbers have been issued, to do this please use: M. Saeidijavash, J. Garg, B. P. Grady, B. Smith, Z. Li, R. J. Young, F. Tarranum and N. Bel Bekri, *Nanoscale*, 2017, DOI: 10.1039/C7NR04686C.

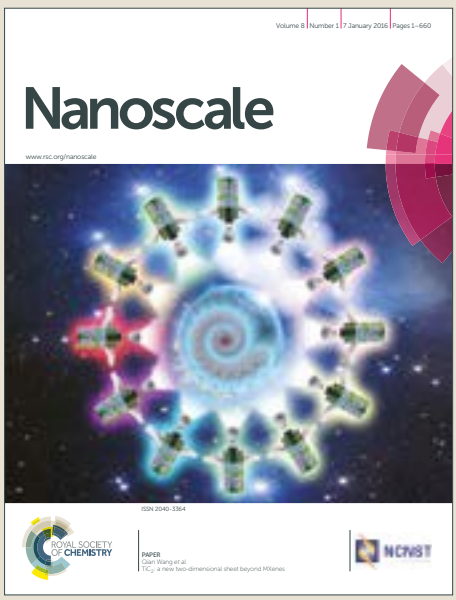

ROYAL SOCIETY OF CHEMISTRY

rsc.li/nanoscale

View Article Online
DOI: 10.1039/C7NR04686C

High thermal conductivity through simultaneously aligned polyethylene lamellae and graphene nanoplatelets

Mortaza Saeidijavash[†], Jivtesh Garg[†], Brian Grady[‡], Benjamin Smith[§], Zheling Li[‖], Robert J. Young[‖], Fatema Tarannum[†], Nour Bel Bekri[†]

† School of Aerospace and Mechanical Engineering, University of Oklahoma, Norman, OK 73019, USA

‡ Chemical, Biological and Materials Engineering, University of Oklahoma, Norman, OK 73019, USA

§ Vision Sciences, University of California, Berkeley, CA 94720, USA

‖ National Graphene Institute and School of Materials, University of Manchester, Manchester M13 9PL, UK

View Article Online
DOI: 10.1039/C7NR04686C

ABSTRACT

The effect of simultaneous alignment of polyethylene (PE) lamellae and graphene nanoplatelets (GnP) on thermal conductivity (*k*) of PE-GnP composites is investigated. Measurements reveal a large increase of 1100% in *k* of the aligned PE-GnP composite using 10 weight% GnPs relative to unoriented pure PE. Rate of increase of *k* with applied strain for the pure PE-GnP composite with 10 wt% GnP is found to be almost a factor of two higher than the pure PE sample, pointing to the beneficial effect of GnP alignment on *k* enhancement. Aligned GnPs are further found to be 3 times as effective in enhancing *k* as in the randomly oriented configuration. Enhancement in *k* is correlated with alignment of PE lamellae and GnPs through wide-angle X-ray scattering and polarized Raman spectroscopy. At the maximum applied strain of 400% and using 10 wt% GnPs, a composite *k* of 5.9 W/mK is achieved. These results demonstrate the large potential of simultaneous alignment effects in achieving high *k* polymer composites.

KEYWORDS: Alignment, polyethylene, graphene, thermal conductivity enhancement

Polymer heat exchangers[1,2] based on polymers such as polyethylene and polypropylene are widely used in applications including water desalination[3,4], solar energy harvesting[5], automotive control units[6] and micro-electronics cooling[7-10]. Polymers offer several advantages such as lower cost and weight which make them more economically competitive compared with metallic heat exchangers[1]. Polymeric materials, however, have much lower intrinsic thermal conductivity[11], *k*, (<0.5 W/mK) compared to metals (> 20 W/mK) which limits their more widespread applicability in thermal management technologies. As means to achieve high *k*

View Article Online
DOI: 10.1039/C7NR04686C

polymers, alignment of polymer chains has emerged as a new and growing field of research. Recently *k* of a single PE fiber with ultra-aligned PE chains was measured to be 104 W/mK almost 200 times[12] larger than *k* of bulk PE (~0.5 W/mK). In another report, effect of alignment of polymer chains was used to achieve thermal conductivity of ~16 W/mK in polyethylene films at draw ratios approaching ~100[13]. Similarly, alignment of filler material has been explored in the past to enhance *k*. In recent work magnetic GnP-Fe_3O_4 hybrids at volume fractions of less than 1 % were aligned through a magnetic field in epoxy composites[14]. Aligned GnP-Fe_3O_4 were found to enhance epoxy *k* by almost 40% relative to epoxy with randomly oriented GnPs. In this work only the GnPs were aligned. Other works have also explored alignment of GnPs through electric field[15,16], flow-assisted alignment[17] as well as self-alignment[18-20]. Large enhancements in *k* through alignment of either the PE chains or filler material suggest that by combining the *k*-enhancements through alignment of both the polymer chains and the GnPs, even larger *k* values can be achieved.

Graphitic nanoplatelets (GnPs) with the thickness in the range of ~10-100 nm are excellent heat conductors with in-plane *k*~1500 W/mK at room temperature[21-23]. GnPs also show lower thermal boundary resistance (TBR)[24] with polymers relative to carbon nanotubes (CNT). TBR between CNTs and polymer matrix is estimated to be in the range of 10^{-8} – 10^{-7} m^2K/W[25]; the corresponding value for GnPs is in the range of 10^{-9} m^2K/W[24]. This lower TBR has led to a significant growth in use of GnPs as filler material to increase thermal conductivity of a polymer. While in-plane *k* of GnPs is very high (~1500 W/mK), it should be noted that the through thickness value is much lower of the order of ~10-20 W/mK[26]. Alignment achieves full advantage of the high in-plane *k* of GnPs. Similarly, by aligning polymer chains, advantage can be taken of the highly efficient heat transfer along their chain axis.

View Article Online
DOI: 10.1039/C7NR04686C

In this work effectiveness of such simultaneous alignment in enhancing thermal conductivity is explored. Alignment of both the polymer chains and embedded GnPs is achieved through application of mechanical strain to the PE-GnP composites. Mechanical strain is known to align the polymer chains in crystallites along the direction of applied strain[27] enhancing k along it (Figs. 1a and b). Similarly, strain has also been shown to align the embedded filler material (Fig. 1c) such as carbon nanotubes[28]. Alignment of GnPs in this work is characterized using laser scanning confocal microscopy and polarized Raman spectroscopy. Alignment of PE crystallites is measured using wide-angle X-ray scattering (WAXS) analysis.

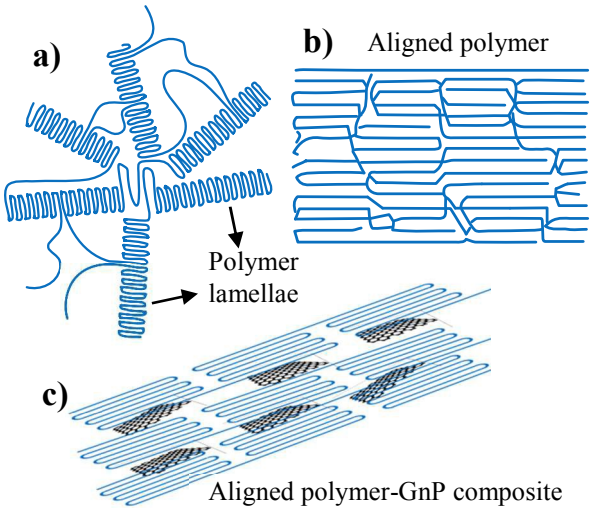

Figure. 1 a) Randomly oriented polymer lamellae in a semi-crystalline polymer b) Alignment induced by strain c) Aligned polymer-GnP composite.

View Article Online
DOI: 10.1039/C7NR04686C

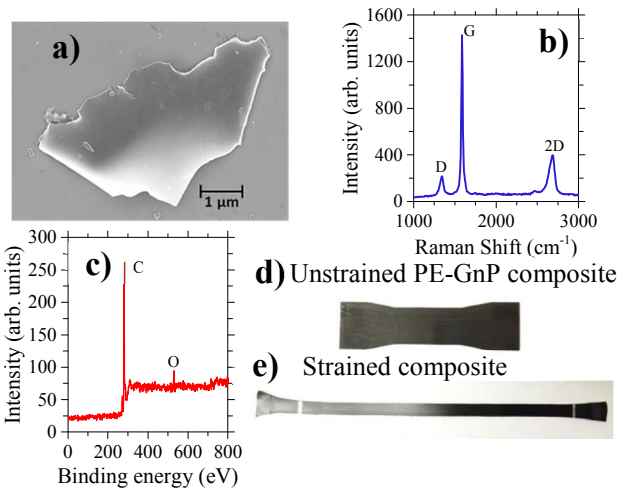

Figure 2 a) SEM image of a typical graphene nanoplatelet used in the study b) Raman and c) XPS analysis of GnPs. d) Unstrained and e) strained PE-GnP composite.

While GnPs are chosen both because of their high intrinsic *k* and better thermal interaction with the polymer matrix, PE is chosen as the base polymer because it exhibits large change in *k* upon alignment[12,13]. The GnPs used in this work are about ~5 µm (Fig. 2a) in lateral size and ~60 in average thickness. They were produced through mechanical cleavage of raw graphite and have relatively low defect density. This is seen in the Raman analysis as a low intensity of the D peak (Fig. 2b). Oxygen content of used GnPs was measured to be less than 2.9% through X-ray photoelectron spectroscopy (Fig. 2c). The polymer matrix used in this work was high density polyethylene with a melt index of 2.2 g/10 min and with a molecular weight of Mn~10600. PE-GnP composites were prepared by melt-compounding[29-31] PE pellets and GnP nanopowder together in a DSM-5 micro-compounder. A mixing time of 40 min and a mixing temperature of 200 °C were used while preparing the composite through melt-compounding. The resulting nanocomposite was then compression-molded to achieve the composite samples with a thickness of ~ 1 mm. GnPs used in this work are not functionalized; the interaction between GnPs and polymer matrix is therefore through van der Walls forces.

Mechanical strain was applied to the composite samples using a motorized slide to induce alignment of the graphene nanoplatelets and polymer chains. The use of low draw rates (~40µm/min) coupled with heating the sample to 60-70 °C during the drawing process prevented

View Article Online
DOI: 10.1039/C7NR04686C

brittle failure and allowed total strains of up to 400% to be achieved. Figure 2d and e show an unstrained and strained PE-GnP composite respectively.

Thermal conductivity of both the unstrained and strained composites was measured through the measurement of thermal diffusivity (α), specific heat capacity (c_p) and density (ρ), using the relation $k = \rho c_p \alpha$. The specific heat capacity of composites was measured using a TA instruments Q-2000 differential scanning calorimeter. Density of samples was measured using Archimedes principle. Thermal diffusivity was measured using the Angstrom method[32] by applying a sinusoidal heat signal at one end of the sample and measuring temperature (T) response at two different locations along the sample. The accuracy of measurement set-up was established through the good agreement between measured k of the pristine PE (0.5 W/mK, Fig. 3a) and that reported in literature[11].

The measured thermal conductivities of pure PE and PE-GnP composites as a function of applied strain ($\varepsilon = \Delta l/l_o$, where Δl is the change in sample length and l_o is the original length) are

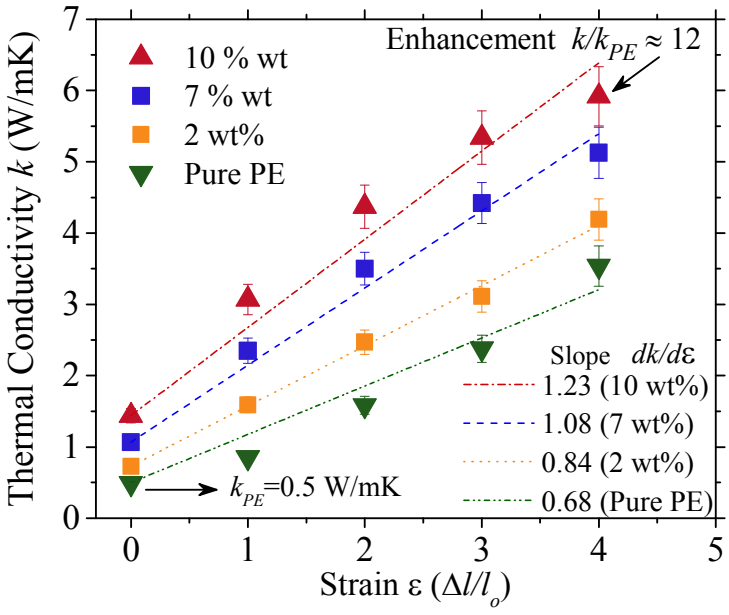

Figure. 3 Measured thermal conductivities of pure PE and PE-GnP composite as a function of applied strain. A highest k of 5.9 W/mK is achieved representing a 12-fold improvement over pristine PE. Increasing slopes of linear-fits point to the role of aligned GnPs in enhancing k

View Article Online
DOI: 10.1039/C7NR04686C

shown in Fig. 3. Thermal conductivities of both pure PE sample and the composite samples increase with applied strain due to alignment of PE chains and embedded GnPs. An extraordinary increase in k for aligned PE-GnP composites can be observed. At the highest strain of ε=4, a k value of 5.9 W/mK is achieved for the aligned PE-GnP composite with 10 wt% GnP. This represents a k-enhancement of almost 1100% relative to the unoriented pure PE matrix (k~0.5 W/mK). In addition, k of the 7 wt% composite at a strain of $\varepsilon = 4$ is measured to be 5.1 W/mK, almost 5 times higher compared to the value for the unstrained composite ($\varepsilon = 0$), k = 1.1 W/mK. These results show significant enhancements in k of the aligned versus the unoriented composites and point to the large potential of alignment effects in yielding high k polymeric materials. The results provide the first evidence that simultaneous alignment effects can provide large enhancements in composite k.

While above values provide an estimate of the absolute k-enhancement in aligned systems, direct evidence of the beneficial effect of aligned GnPs in enhancing k is gained by comparing the slopes of the best-fit lines for the three samples. For the pure PE sample, a slope of k-increase with respect to applied strain is found to be $(dk/d\varepsilon)_{\text{pure-PE}} \approx 0.67$. In the pure PE sample, this k enhancement with respect to applied strain is solely due to alignment of PE chains and has been well studied before[33]. As 7 wt% GnPs are added to the sample, the slope increases to $(dk/d\varepsilon)_{\text{composite}} \approx 1.03$. In the composite sample, k-enhancement with applied strain is through alignment of both PE chains and GnPs. The larger slope is a direct manifestation of the beneficial effect of aligned GnPs in enhancing composite k (if the aligned GnPs did not cause any additional increase in k relative to randomly oriented GnPs, the only effect responsible for k-increase with respect to applied strain in the composite would be the alignment of PE chains, this would have resulted in the same slope as that of pure PE sample assuming that the alignment of

View Article Online
DOI: 10.1039/C7NR04686C

the PE was the same in the pure and composite samples). As the weight fraction of GnPs in the composite is increased to 10 wt%, the slope increases to $(dk/d\varepsilon)_{composite} \approx 1.24$. This points to the enhanced effect of alignment of larger quantities of the GnPs within the composite. This almost a factor of two higher rate of *k*-increase with applied strain in the PE-GnP (10 wt%) composite relative to the pure PE sample is due to the cumulative contributions of alignment of PE chains and GnPs to *k* enhancement and clearly points to the promise of such simultaneous alignment in enhancing composite *k*.

Quantitative estimate of the effectiveness of aligned versus randomly oriented GnPs can also be achieved by comparing the difference between the thermal conductivity values of the pure PE sample and composite at the same strain. At zero strain, the difference between the two is due to randomly oriented GnPs. At higher strains, the difference between the two *k* values is through GnPs which are now aligned providing a direct comparison of the k enhancement between aligned GnPs and randomly oriented GnPs. For the 7 wt% sample the enhancement at zero strain is $k_{composite}^{\varepsilon=0} - k_{PE}^{\varepsilon=0} = 0.5$ W/mK. As the strain is increased to $\varepsilon = 3$, the difference becomes $k_{composite}^{\varepsilon=3} - k_{PE}^{\varepsilon=3} = 1.7$ W/mK. Comparing these two enhancement values, aligned GnPs are found to be more than 3 times as effective as randomly oriented GnPs in enhancing thermal conductivity. Similar results are found comparing enhancements for the 10 wt% sample. This analysis clearly demonstrates the increased effectiveness of GnPs in enhancing *k* in aligned form

Table 1: Thermal conductivity enhancement through alignment effects

Sample composition	*k* (W/mK)	Fraction	Alignment Method	Reference
Aligned GnP/epoxy	0.45	1.05 vol%	Electric field	15
Aligned-interconnected GnP/PDMS[ǂ]	2.13	0.92 vol%	Freeze casting of self-aligned GO[#] liquid crystal	18
Aligned GnP/epoxy	0.6	1 vol%	Magnetic field	14
Aligned GnP/epoxy	0.37	0.52 vol%	Magnetic field	34
Aligned GO[#]/cellulose	6.17 (3.56)	30 wt% (10 wt%)	Self-alignment	19
Aligned GnP/PDMS[ǂ]	6.05 (1.04)	20 vol% (7.5 vol%)	Electric field	16
Aligned GnP/PVDF[ך]	10 (1.06)	25 vol% (5 vol%)	Flow induced	17
Aligned GnP/Aligned PE	5.9	10wt% (6.2 vol%)	Mechanical strain	This work

ǂPDMS: Polydimethylsiloxane ךPVDF: Polyvinylidene fluoride #GO: Graphene Oxide

View Article Online
DOI: 10.1039/C7NR04686C

versus randomly oriented configuration.

We further compare effectiveness of mechanical strain mediated alignment in enhancing *k* with that through other means such as electric field. In Table 1 we compare the results of *k*-enhancement through GnPs aligned by different techniques[14-19,34,35]. In the first study in Table 1, GnPs with volume fractions of up to ~ 1.08 % were aligned through electric field in epoxy composites[15]. At low volume fractions ~0.6%, *k*-enhancement through aligned GnPs was almost twice that due to randomly oriented case. At higher volume fractions (~1 %), however, effectiveness of electric field in aligning GnPs diminished due to presence of GnP agglomerates, leading to smaller *k*-enhancements. Alignment of only low volume fractions (< 1 vol%) limited the highest *k* value achieved to 0.45 W/mK. In this work, we find that *k*-enhancements for 7 wt% and 10 wt% GnP content are proportional to the volume fractions, indicating no decrease in the ability of mechanical strain to align greater quantities of GnPs. This points to the advantages of mechanical strain relative to electric field in achieving higher thermal conductivity values. The results suggest that even higher *k* values can be achieved through alignment of larger quantities of GnP using mechanical strain induced alignment.

Aligned GnPs are also found to be more effective in enhancing *k* relative to aligned CNTs through comparison with previously reported results on aligned PVA (poly vinyl alcohol)-CNT composites.[36] For the 10 wt% CNT composite and at a strain of 4.5, aligned CNTs were found to enhance thermal diffusivity by $\alpha_{PVA-CNT}^{\varepsilon=4.5} - \alpha_{PVA}^{\varepsilon=4.5} = 0.55$ mm^2/s relative to pure PVA (at the same strain of 4.5) in the PVA-CNT composites. In this work, the same comparison for 10 wt% GnP composite yields an enhancement of $\alpha_{PE-GnP}^{\varepsilon=4.0} - \alpha_{PE}^{\varepsilon=4.0} = 1.13$ mm^2/s through the use of aligned GnPs. Aligned GnPs are thus found to be twice as effective in enhancing *k* as aligned CNTs.

View Article Online
DOI: 10.1039/C7NR04686C

Above comparisons shed light on the advantages of mechanical strain and use of GnPs for alignment mediated thermal conductivity enhancement. We next show that simultaneous alignment of polymer lamellae and GnPs provides higher *k* enhancement than achievable through alignment of GnPs alone. In Table 1 we further compare *k*-enhancement through alignment of GnPs induced by techniques such as magnetic field, flow processes and self-alignment with the present work. For each study, we present the highest *k* achieved, and also the *k* values at volume fractions close to the 6.2 vol% used in this study (volume fraction for the 10 wt% composition is ~ 6.2 vol%, determined through density measurements). Comparison with these works clearly shows that *k* value achieved in this work (5.9 W/mK) through simultaneous alignment of PE chains and GnPs (10 wt%) is significantly higher than achieved through alignment of GnPs alone at similar compositions. These comparisons shed light on the large potential of simultaneous alignment effects in developing high *k* polymeric composites.

View Article Online
DOI: 10.1039/C7NR04686C

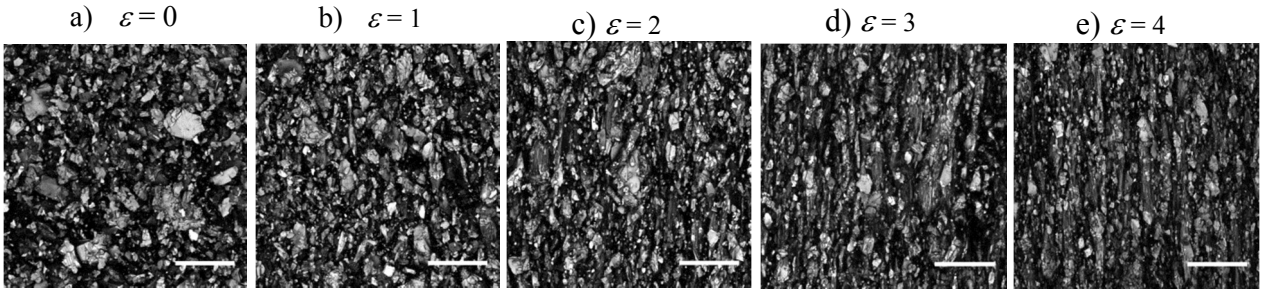

Figure. 4 Confocal microscopy images of GnPs in 7 wt% PE-GnP composite sample for different applied strains (ε) of a) 0, b) 1, c) 2, d) 3 and e) 4. Increasing alignment of GnPs with increasing strain is clearly visible in above maximum intensity projections. Scale bar = 20 μm.

To analyze the influence of GnP alignment on the composite thermal properties, the degree of its alignment must be determined. Alignment of GnPs within the nanocomposite was analyzed in

View Article Online
DOI: 10.1039/C7NR04686C

this work through the use of laser scanning confocal microscopy[37] (LSCM) and polarized Raman spectroscopy. While LSCM provides a visual understanding of GnP alignment, polarized Raman allows a quantitative estimate of the graphene orientation. LSCM generates optical sections as thin as 300 nm axially by using reflected light to create images while blocking out any out-of-focus light. By collecting a series of these optical sections along the optical axis one can generate a 3D reconstruction of a volume within an intact specimen. In this work, we use a Leica SP8

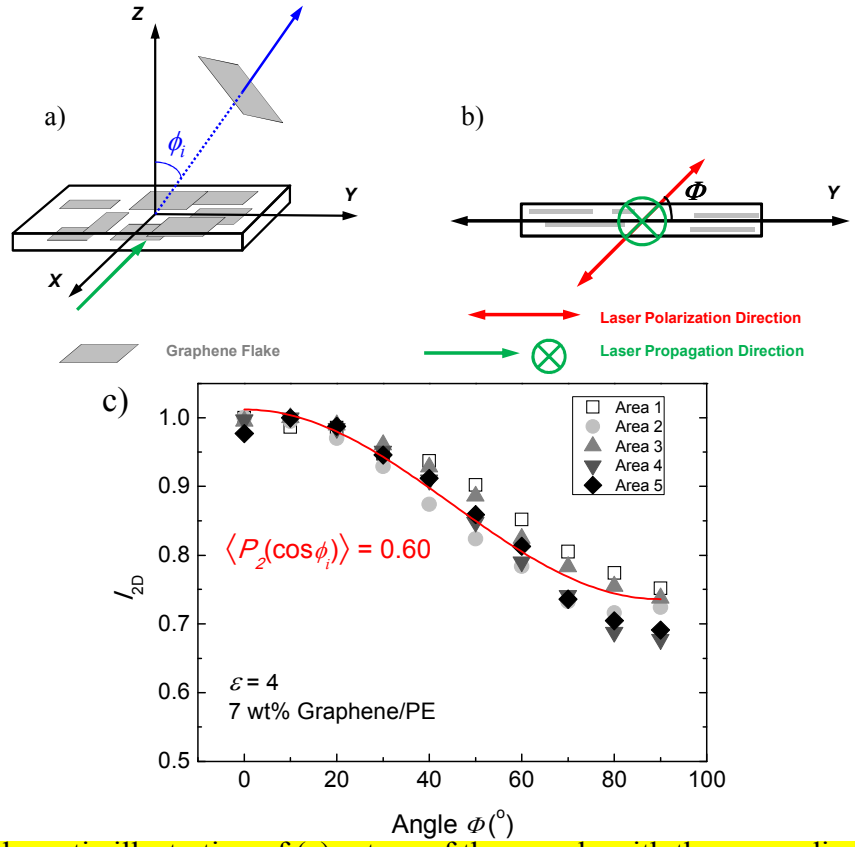

Figure. 5 Schematic illustration of (a) set-up of the sample with three coordinates defining the spatial position of a graphene flake, and also with the laser propagation direction. ϕ_i is the angle between the surface normal of the sample and the surface normal of an arbitrary flake; (b) side view along the X axis, Φ is the angle between the laser polarization direction and the Y axis, c) I_{2D} as a function of Φ of five areas of the 7wt% graphene/PE sample with a strain of 4. The red line corresponds to the curve fitting of all the points from the 5 different areas.

laser scanning confocal microscope with a 561 nm diode pumped solid state (DPSS) laser. The samples are imaged with a 63×/1.4 oil immersion objective with the pinhole aperture at 0.2 airy

View Article Online
DOI: 10.1039/C7NR04686C

units (AU) and voxel dimensions of 120 nm × 120 nm × 120 nm. The image volume for each sample was 246 μm × 246 μm × 10 μm with three images per sample. Fig. 4 shows LSCM maximum intensity projections of GnPs in unstrained nanocomposite sample (7 wt% GnP) and same composition sample with strains (ε) of 1, 2, 3 and 4. While GnPs are seen to be randomly oriented in Fig. 4a for the unstrained sample, increasing alignment of GnPs with increasing applied strain is clearly visible in Figs. 4 b, c,d and e. These LSCM images visually demonstrate alignment of GnPs upon application of strain.

Absolute alignment of GnPs in terms of their angle of orientation is also measured using polarized Raman spectroscopy. The Raman spectra were taken using a Renishaw inVia Reflex Spectrometer System, equipped with a laser with wavelength λ= 532 nm. To measure orientation using polarized Raman we used the 7wt% graphene/PE sample with a strain of ε=4. The sample was set up with the laser illuminating along the *X* direction, as shown in Fig. 5(a). Orientation of GnPs is described by the angle ϕ_i between the surface normal of the composite sample and the surface normal of an arbitrary GnP flake (Fig. 5(a)). The angle between the incident laser polarization and the *Y* axis when viewed along *X* axis, is defined as Φ (Fig. 5(b)). The scattered radiation was not polarized in this work. During the measurement, the incident laser polarization was rotated, while the sample was kept fixed. The intensity of the Raman 2D band (I_{2D}) as a function of Φ measured at five areas is shown in Fig. 5(c). For each area, the intensity values at different Φ were normalized to the maximum. To quantify the orientation of GnPs, the model in Ref.[38] is modified to account for absence of polarization of scattered radiation in this work. The modified model is used to express the Raman intensity as a function of angle Φ and the parameter $\langle P_2(\cos\phi_i)\rangle$ as below,

View Article Online
DOI: 10.1039/C7NR04686C

$$I_{2D}(\Phi) = I_0\left\{\frac{2}{3} - \frac{1}{2}\cos^2\Phi + \langle P_2(\cos\phi_i)\rangle\left(-\frac{2}{3} + \cos^2\Phi\right)\right\} \quad (1)$$

where I_o is the amplitude. $\langle P_2(\cos\phi_i)\rangle$ describes the average orientation of GnPs through the relation $\langle P_2(\cos\phi_i)\rangle = \{3\langle\cos^2\phi_i\rangle - 1\}/2$, where $\langle\cos^2\phi_i\rangle$ is the average value of $\cos^2\phi_i$. By fitting the measured result to Eq. (1), $\langle P_2(\cos\phi_i)\rangle$ can be obtained, as an indication of the spatial orientation of GnPs as shown in Fig. 5c. Values of $\langle P_2(\cos\phi_i)\rangle$ are 0 and 1 for random and completely aligned orientations respectively (corresponding values of $\langle\cos^2\phi_i\rangle$ are 0.33 and 1.0). The value of $\langle P_2(\cos\phi_i)\rangle$ obtained by fitting Eq. (1) to the measured intensity data is achieved to

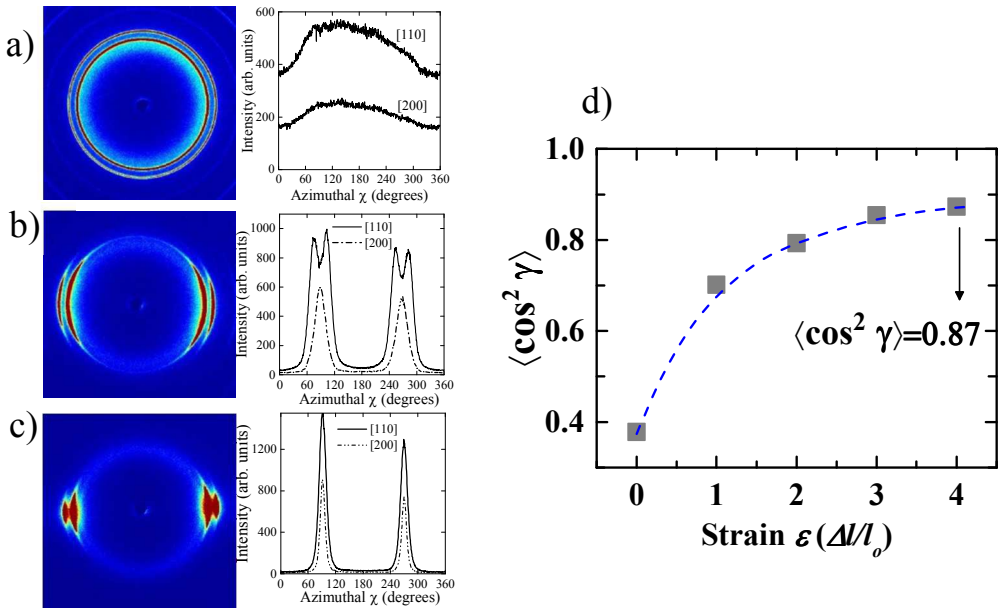

Figure. 6 a), b) and c) WAXS patterns for strains of 0, 2 and 4, in the pure PE sample d) Average orientation of PE chains in crystallites with respect to draw direction.

be 0.6 (Fig. 5c). This large value ($\langle\cos^2\phi_i\rangle \sim 0.73$) indicates a high level of GnP alignment in the strained composite sample. We find that this orientation level of GnPs is comparable to the alignment of PE crystallites discussed next.

View Article Online
DOI: 10.1039/C7NR04686C

While above measurements shed light on alignment of GnPs, alignment of crystalline PE chains is measured through wide-angle X-ray diffraction measurements (WAXS). Through WAXS, the average relative orientation of the PE chains in crystallites with respect to the stretch direction is measured in terms of $\langle \cos^2 \gamma \rangle$ (the average value of $\cos^2 \gamma$) where γ is the angle between the PE chain axis and draw direction. The WAXS patterns in pure PE sample obtained for different strains are shown in Fig. 6 a, b, and c. The 2D patterns clearly show alignment effects; upon stretching, the rings become arcs in WAXS spectra[39]. The obtained intensities from these plots are integrated to compute the average orientation $\langle \cos^2 \gamma \rangle$, giving the alignment of PE chains in crystallites with respect to stretch direction. The value of $\langle \cos^2 \gamma \rangle$ is presented in Fig. 6(d) where increasing value of $\langle \cos^2 \gamma \rangle$ with increasing strain indicates increasing alignment. A high degree of PE alignment at the largest strain (ε=4) is indicated by a large value of $\langle \cos^2 \gamma \rangle$ = 0.87.

WAXS measurements were also performed on the 7 wt% composite sample for strain ε=4 to compare PE alignment levels with the pure PE samples. The value of $\langle \cos^2 \gamma \rangle$ was identical to the one obtained for pure PE sample, indicating that PE chain orientation is identical in the composite and pure PE sample for the same applied strain. This also implies that the small GnP content of 4.4 vol% (for the 7 wt% sample) does not impact alignment of polymer lamellae.

We further use Raman and WAXS alignment measurements to extract relative contributions of aligned PE chains and GnPs to total *k*-enhancement. For 10 wt% filler content, increasing the strain from ε=0 to ε=2 leads to a total *k*-enhancement of 2.9 W/mK (Fig. 3). Contribution of alignment of PE chains to this is be taken to be the same as in the pure PE sample, 1.1 W/mK from the difference between *k* values of pure PE sample for ε=2 and ε=0. This is due to same PE alignment in both the composite and pure PE sample (as shown by the

View Article Online
DOI: 10.1039/C7NR04686C

above WAXS measurements). The further enhancement induced in composite *k* due to alignment of GnPs is thus 1.8 W/mK (obtained by subtracting the PE contribution from total enhancement). For strain of ε=3, the total *k*-enhancement reaches 3.9 W/mK. The contributions of aligned PE chains and aligned GnPs to this are estimated to be 1.9 and 2.0 W/mK respectively. These near equal contributions of alignment of PE and GnPs to total *k*-enhancement lead to an almost doubling of the slope of *k*-increase with strain for the 10 wt% composite relative to pure PE sample and yield overall *k*-value of 5.9 W/mK These results provide the first proof that strain induced higher *k*-enhancement via mechanical stretching can occur through combined contributions of alignment of polymer matrix and the embedded graphitic nanoplatelets and may provide new pathways to achieving high *k* polymeric materials.

It should be noted that alignment levels presented in this work can be realized on a bulk scale through widely used manufacturing processes such as polymer extrusion. In the past extrusion has been found to align both polyethylene[40] and polypropylene[41,42] chains. Alignment of filler material such as CNTs[43,44] and GnPs[45] upon extrusion has also been reported. Simultaneous alignment of polymer chains and high *k* filler material such as GnPs through composite extrusion may lead to inexpensive and scalable methods for processing of high thermal conductivity polymer composites.

In summary, we have demonstrated the effect of strain induced simultaneous alignment of PE chains and GnPs on *k*-enhancement of PE-GnP composites. These composites were prepared by melt-compounding PE pellets and GnPs. GnP weight fractions of up to 10% were included in the study. Both laser scanning confocal microscopy and polarized Raman spectroscopy demonstrated high level of GnP alignment in strained samples. Similarly, wide-angle X-ray scattering measurements revealed the alignment of PE chains. At the highest strain of 400% and

View Article Online
DOI: 10.1039/C7NR04686C

for 10 wt% GnP composition an overall thermal conductivity of 5.9 W/mK was achieved representing an 1100% enhancement over the *k* of unoriented pristine PE (0.5 W/mK). Aligned GnPs were found to be 3 times as effective in enhancing *k* as randomly oriented GnPs. Similar comparison with aligned CNTs showed the aligned GnPs to be twice as effective as aligned CNTs in enhancing composite *k*. These results shed light on the large potential of simultaneous alignment effects in enhancing *k* and provide new avenues for developing high *k* polymeric composites.

Corresponding Author

Email: garg@ou.edu

Conflicts of Interest

There are no conflicts of interest

REFERENCES

1 Chen, X., Su, Y., Reay, D. & Riffat, S. Recent Research developments in polymer heat exchangers-A review. *Renewable and Sustainable Energy Reviews* **60**, 1367 (2016).
2 Reay, D. A. The use of polymers in heat exchangers. *Heat Recovery Systems and CHP* **9**, 209 (1989).
3 Dreiser, C., Kratz, L. J. & Bart, H.-J. in *International Conference on Heat exchanger fouling and cleaning.* (ed H. Muller-Steinhagen and A.P. Watkinson M.R. Malayeri) 296.
4 El-Dessouky, H. T. & Ettouney, H. M. Plastic/compact heat exchangers for single-effect desalination systems. *Desalination* **122**, 271 (1999).
5 Liu, W., Davidson, J. & Mantell, S. Thermal analysis of polymer heat exchangers for solar water heating: A case study. *Journal of solar energy engineering* **122**, 84 (2000).
6 Mallik, S., Ekere, N., Best, C. & Bhatti, R. Investigation of thermal management materials for automotive electronic control units. *Applied Thermal Engineeering* **31**, 355 (2011).
7 Procter, P. & Solc, J. Improved Thermal Conductivity in Microelectronic Encapsulants. *IEEE Transactions on Components, Hybrids, and Manufacturing Technology* **14**, 708 (1991).
8 Lu, X. & Xu, G. Thermally Conductive Polymer Composites for Electronic Packaging. *Journal of Applied Polymer Science* **65**, 2733 (1997).
9 Lin, Z., Liu, Y., Moon, K. & Wong, C. in *Electronic components and Technology Conference* 1692 (2013).

View Article Online
DOI: 10.1039/C7NR04686C

10 Lin, Z., Yao, Y., Mcnamara, A., Moon, K. & Wong, C. P. in *Electronic components and Technology Conference* 1437 (2012).
11 Yu, J., Sundqvist, B., Tonpheng, B. & Andersson, O. Thermal conductivity of highly crystallized polyethylene. *Polymer* **55**, 195 (2014).
12 Shen, S., Henry, A., Tong, J., Zheng, R. & Chen, G. Polyethylene nanofibres with very high thermal conductivities *Nature Nanotechnology* **5**, 251-255 (2010).
13 Ghasemi, H., Thoppey, N., Huang, X., Loomis, J., Li, X., Tong, J., Wang, J. & Chen, G. in *14th IEEE ITHERM Conference* (Orlando, FL, 2014).
14 Yan, H., Tang, Y., Long, W. & Li, Y. Enhanced thermal conductivity in polymer composites with aligned graphene nanosheets. *J. Mater. Sci.* **49**, 5256 (2014).
15 Wu, S., Ladani, R. B., Zhang, J., Bafekrpour, E., Ghorbani, K., Mouritz, A. P., Kinloch, A. J. & Wang, C. H. Aligning multilayer graphene flakes with an external electric field to improve multifunctional properties of epoxy nanocomposites. *Carbon* **94**, 607 (2015).
16 Guo, Y., Chen, Y., Wang, E. & Cakmak, M. Roll-to-Roll continuous manufacturing multifunctional nanocomposites by electric-field-assisted "Z" direction alignment of graphite flakes in poly(dimethysiloxane). *ACS Appl. Mater. Interfaces* **9**, 919 (2017).
17 Jung, H., Yu, S., Bae, N., Cho, S., Kim, R. H., Cho, S. H., Hwang, I., Jeong, B., Ryu, J. S., Hwang, J., Hong, S. M., Koo, C. M. & Park, C. High through-plane thermal conduction of graphene nanoflake filled polymer composites melt-processed in an L-shape kinked tube. *ACS Appl. Mater. Interfaces* **7**, 15256 (2015).
18 Lian, G., Tuan, C.-C., Li, L., Jiao, S., Wang, Q., Moon, K. S., Cui, D. & Wong, C.-P. Vertically aligned and interconnected graphene networks for high thermal conductivity of epoxy composites with ultralow loading. *Chem. Mater.* **28**, 6096 (2016).
19 N.Song, Jiao, D., Ding, P., Cui, S., Tang, S. & Shi, L. Anisotropic thermally conductive flexible films based on nanofibrillated cellulose and aligned graphene nanosheets. *J. Mater. Chem. C* **4**, 305 (2016).
20 Zhao, W., Kong, J., Liu, H., Zhuang, Q., Gu, J. & Guo, Z. Ultra-high thermally conductive and rapid heat responsive poly (benzobisoxazole) nanocomposites with self-aligned graphene. *Nanoscale* **8**, 19984 (2016).
21 Balandin, A. A., Ghosh, S., Bao, W., Calizo, I., Teweldebrhan, D., Miao, F. & Lau, C. N. Superior thermal conductivity of single-layer graphene. *Nano Letters* **8**, 902 (2008).
22 Ghosh, S., Bao, W., Nika, D. L., Subrina, S., Pokatilov, E. P., Lau, C. N. & Balandin, A. A. Dimensional crossover of thermal transport in few-layer graphene. *Nature Materials* **9**, 555 (2010).
23 Fugallo, G., Cepellotti, A., Paulatto, L., Lazzeri, M., Marzari, N. & Mauri, F. Thermal conductivity of graphene and graphite: Collective excitations and mean free paths. *Nano Letters* **14**, 6109 (2014).
24 Shahil, K. M. F. & Balandin, A. A. Graphene-Multilayer graphene nanocomposites as highly efficient thermal interface materials. *Nano Letters* **12**, 861 (2012).
25 Huxtable, S. T., Cahill, D. G., Shenogin, S., Xue, L., Ozisik, R., Barone, P., Ursey, M., Strano, M. S., Siddons, G., Shim, M. & Keblinski, P. Interfacial heat flow in carbon nanotube suspensions. *Nature Materials* **2**, 731 (2003).
26 Balandin, A. A. Thermal properties of graphene and nanostructured carbon materials. *Nature Materials* **10**, 569 (2011).

View Article Online
DOI: 10.1039/C7NR04686C

27 Aggarwal, S. L., Tilley, G. P. & Sweeting, O. J. Changes in orientation of crystallites during stretching and relaxation of polyethylene films. *Journal of Polymer science* **51**, 551 (1961).

28 Yao, S. H., .Yuan, J. K., Zhou, T., Dang, Z. M. & Bai, J. Stretch-Modulated Carbon Nanotube Alignment in Ferroelectric PolymerComposites: Charctaerization of the Orientation State and its influence on the dielectric properties. *J. Phys. Chem. C* **115**, 20011 (2011).

29 Potts, J. R., Dreyer, D. R., Bielawski, C. W. & Rwoff, R. S. Graphene based polymer nanocomposites. *Polymer* **52**, 5-25 (2011).

30 Kim, H., Kobayashi, S., AbdurRahim, M. A., Zhang, M. J., Khsainova, A., Hillmyer, M. A., Abdala, A. A. & Macoska, C. W. Graphene/polyethylene nanocomposites: Effect of polyethylene functionalization and blending methods. *Polymer* **52**, 1837-1846 (2011).

31 Ozkoc, G., Bayram, G. & Tiesnitsch, J. Microcompunding of organoclay-ABS/PA6 blend based nanocomposites. *Polymer Composites* **29**, 345-356 (2008).

32 Zhu, Y. Heat-loss modified Angstrom method for simultaneous measurements of thermal diffusivity and conductivity of graphite sheets:The origins ofheat loss in Angstrom method. *International Journal of Hat and Mass Transfer* **92**, 784 (2016).

33 Mergenthaler, D. B. & Pietralla, M. Thermal conductivity in ultra-oriented polyethylene. *Macromolecules* **25**, 3500 (1992).

34 Yan, H., Wang, R., Li, Y. & Long, W. Thermal conductivity of magnetically aligned graphene-polymer composites with Fe_3O_4-decorated graphene nanosheets. *Journal of Electronic Materials* **44**, 658 (2015).

35 Leung, S. N., Khan, M. O., Naguib, H. & Dawson, F. Multifunctional polymer nanocomposites with uniaxially aligned liquid crystal polymer fibrils and graphene nanoplatelets. *Appl. Phys. Lett.* **104**, 081904 (2014).

36 Song, W.-L., Wang, W., Veca, L. M., Kong, C. Y., Cao, M.-S., Wang, P., Meziam, M. J., Qian, H., LeCroy, G. E., Cao, L. & Sun, Y. P. Polymer/carbon nanocomposites for enhanced thermal transport properties - carbon nanotubes versus graphene sheets as nanoscale fillers. *J. Mater. Chem.* **22**, 17133 (2012).

37 Yazdani, H., Smith, B. E. & Hatami, K. Multi-walled carbon nanotube-filled polyvinyl chloride composites: Influence of processing method on dispersion quality, electrical conductivity and mechanical properties. *Composites: Part A* **82**, 65-77 (2016).

38 Li, Z., Young, R. J., Wilson, N. R., Kinloch, I. A., Vallés, C. & Li, Z. Effect of the orientation of graphene-based nanoplatelets upon the Young's modulus of nanocomposites. *Compos. Sci. Technol.* **123**, 125-133, doi:http://dx.doi.org/10.1016/j.compscitech.2015.12.005 (2016).

39 Genetti, W. B., .Lamirand, R. J. & Grady, B. P. Wide-Angle X-ray scattering study of crystalline orientation in reticulatep-doped polymer composites. *Journal of Applied Polymer Science* **70**, 1785 (1998).

40 Nakayama, K. & Kanetsuna, H. Hydrostatic extrusion of solid polymers. *Journal of Materials Science* **10**, 1105 (1975).

41 Wang, C. H. & Cavannaugh, D. B. Effect of chain alignment on the Brillouin scattering spectra of hydrostatically extruded polypropylene. *Macromolecules* **14**, 1061 (1981).

42 Chen, X., Leugers, M. A., Kirch, T. & Stanley, J. Orientation mapping of extruded polymeric composites by polarized micro-raman spectroscopy. *Journal of Spectroscopy* **2015**, 518054 (2015).

View Article Online
DOI: 10.1039/C7NR04686C

43 Sulong, A. B. & Park, J. Alignment of multi-walled carbon nanotubes in a polyethylene matrix by extrusion shear flow: mechanical properties enhancement. *Journal of Composite Materials* **45**, 931 (2010).
44 Rangari, V. K., Yousuf, M., Jeelani, S., Pulikkathara, M. X. & Khabashesku, V. N. Alignment of carbon nanotubes and reinforcing effects in nylon-6 polymer composite fibers. *Nanotechnology* **19**, 245703 (2008).
45 Gaska, K., Xu, X., Gubanski, S. & Kaddar, R. Electrical, mechanical and thermal properties of LDPE graphene nanoplatelets composites produced by means of melt extrusion process. *Polymers* **9**, 11 (2017).